Thermal and Mechanical Influence of a Deep Geological Repository in Crystalline Rock on the Ground Surface

NWMO-TR-2016-15 October 2016

Ruiping Guo

Nuclear Waste Management Organization

nwmo

NUCLEAR WASTE MANAGEMENT ORGANIZATION

SOCIÉTÉ DE GESTION DES DÉCHETS NUCLÉAIRES

Nuclear Waste Management Organization
22 St. Clair Avenue East, 6th Floor
Toronto, Ontario
M4T 2S3
Canada

Tel: 416-934-9814
Web: www.nwmo.ca

Thermal and Mechanical Influence of a Deep Geological Repository in Crystalline Rock on the Ground Surface

NWMO-TR-2016-15

October 2016

Ruiping Guo
Nuclear Waste Management Organization

Document History

Title:	Thermal and Mechanical Influence of a Deep Geological Repository in Crystalline Rock on the Ground Surface		
Report Number:	NWMO-TR-2016-15		
Revision:	R000	Date:	October 2016
Nuclear Waste Management Organization			
Authored by:	Ruiping Guo		
Verified by:	Gobien Mark		
Reviewed by:	Neale Hunt, Alan Murchison, Andre Vorauer, Tom Lam, Sasha Zivkovic		
Approved by:	Paul Gierszewski		

ABSTRACT

Title: **Thermal and Mechanical Influence of a Deep Geological Repository in Crystalline Rock on the Ground Surface**
Report No.: **NWMO-TR-2016-15**
Author(s): Ruiping Guo
Company: Nuclear Waste Management Organization
Date: October 2016

Abstract

This report describes the thermal and mechanical influence of a single level conceptual deep geological repository (DGR) in a hypothetical crystalline host rock geosphere on the ground surface.

Sensitivity studies are performed to investigate the influence of Young's modulus for the rock, the depth of the repository and the convective heat transfer coefficient applied at the ground surface. The influence of the mechanical boundary condition applied on the far-field vertical surfaces is also studied.

For the cases evaluated, the presence of the conceptual DGR does not have any significant influence on the surface temperature. There is a general slow uplift of the ground surface due to thermal expansion over an area larger than the repository footprint, with a maximum uplift of about 28 cm occurring above the centre of the repository in about 3,400 years.

TABLE OF CONTENTS

LIST OF TABLES

Page

LIST OF FIGURES

Page

1. INTRODUCTION

The Adaptive Phased Management (APM) approach for the long-term management of Canada's used nuclear fuel includes placement of the used fuel in engineered excavations around 500 m deep in either crystalline or sedimentary rock.

A series of conceptual design studies for a deep geological repository (DGR) has been carried out in the past (Acres et al. 1985, 1993; Mathers 1985; Tsui and Tsai 1985; Golder Associates Ltd. 1993; Baumgartner et al. 1994; Guo 2007, 2010, 2016; Carvalho and Steed 2012). These studies focus on two- and three-dimensional thermal transient and thermo-mechanical analyses of the materials around repositories.

The purpose of this report is to summarize the approach and findings of a modelling study on the potential thermal and mechanical responses of the ground surface above a 500 m deep DGR, hosted at a hypothetical crystalline rock site and based on the Mark II concept.

This report contains the following:

- A description of the modelled scenarios.
- Material properties used in the models.
- Coupled thermal-mechanical modelling.
- Sensitivity studies to examine the effect of boundary conditions applied on the outside vertical surfaces and the ground surface of the modelled domain, the repository depth, and Young's modulus for the rock.
- Summary and conclusions.

2. DESCRIPTION OF A PROPOSED DEEP GEOLOGICAL REPOSITORY

The conceptual DGR layout to be modelled consists of an array of horizontal rectangular-shaped placement rooms (Noronha, 2016) (Figure 1). The placement room is 2.2 m high, 3.2 m wide and 308 m long.

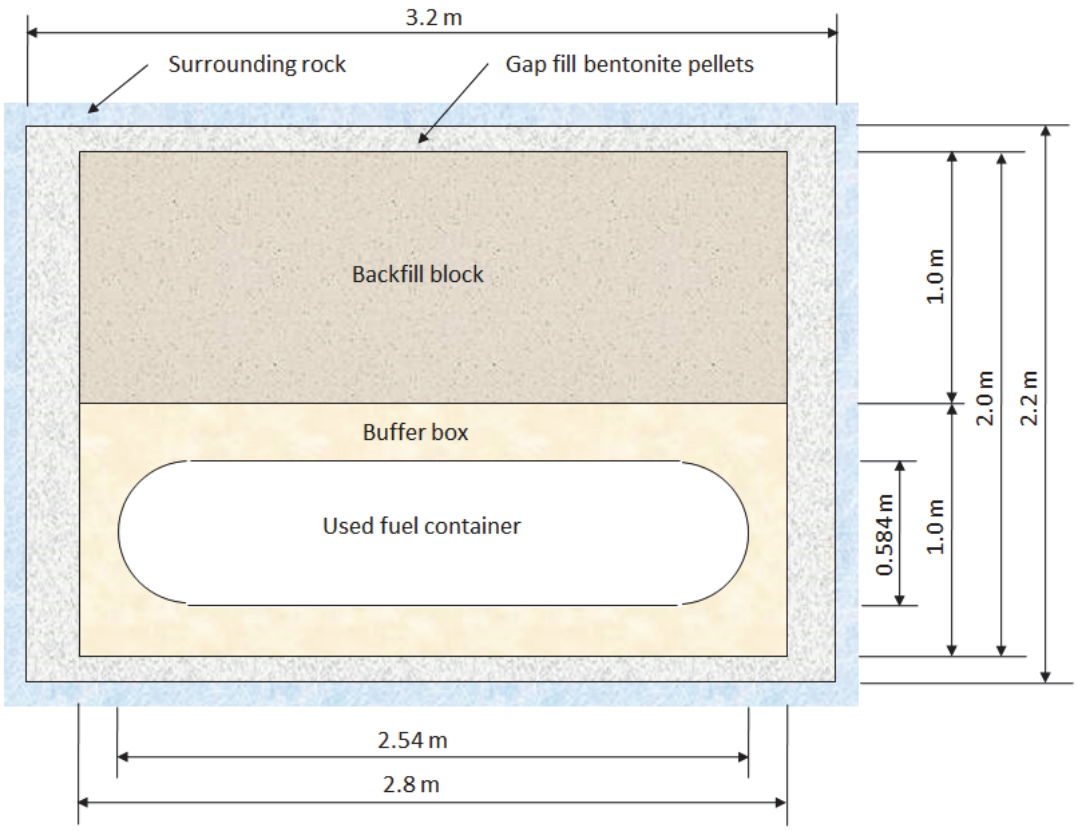

Figure 1: Sectional View of Placement Room

Access tunnels connect the placement rooms for moving personnel, material, excavated rock, used-fuel storage containers and backfilling materials. These rooms are arranged into several distinct sections or panels. Each panel consists of a number of placement rooms (Noronha, 2016) (Figure 2), each room containing a number of Mark II used-fuel containers within two layers. One Mark II used-fuel container is horizontally placed in a bentonite box which is placed perpendicular to the tunnel axis (Figure 1). Between two bentonite boxes is a dense backfill block (Noronha, 2016) (Figure 3). Each Mark II container is 2.8 m long with a diameter of 0.564 m and accommodates 48 used CANDU® fuel bundles. The container design consists of a 3 mm thick copper outer corrosion-barrier and an inner, carbon-steel load-bearing component. The conceptual DGR has a minimum total capacity of about 4.6 million intact fuel bundles or about 96,000 Mark II used-fuel containers (UFCs). Dimensions of the repository, placement room, containers and sealing materials used in this analysis are shown in Figure 1 through Figure 3.

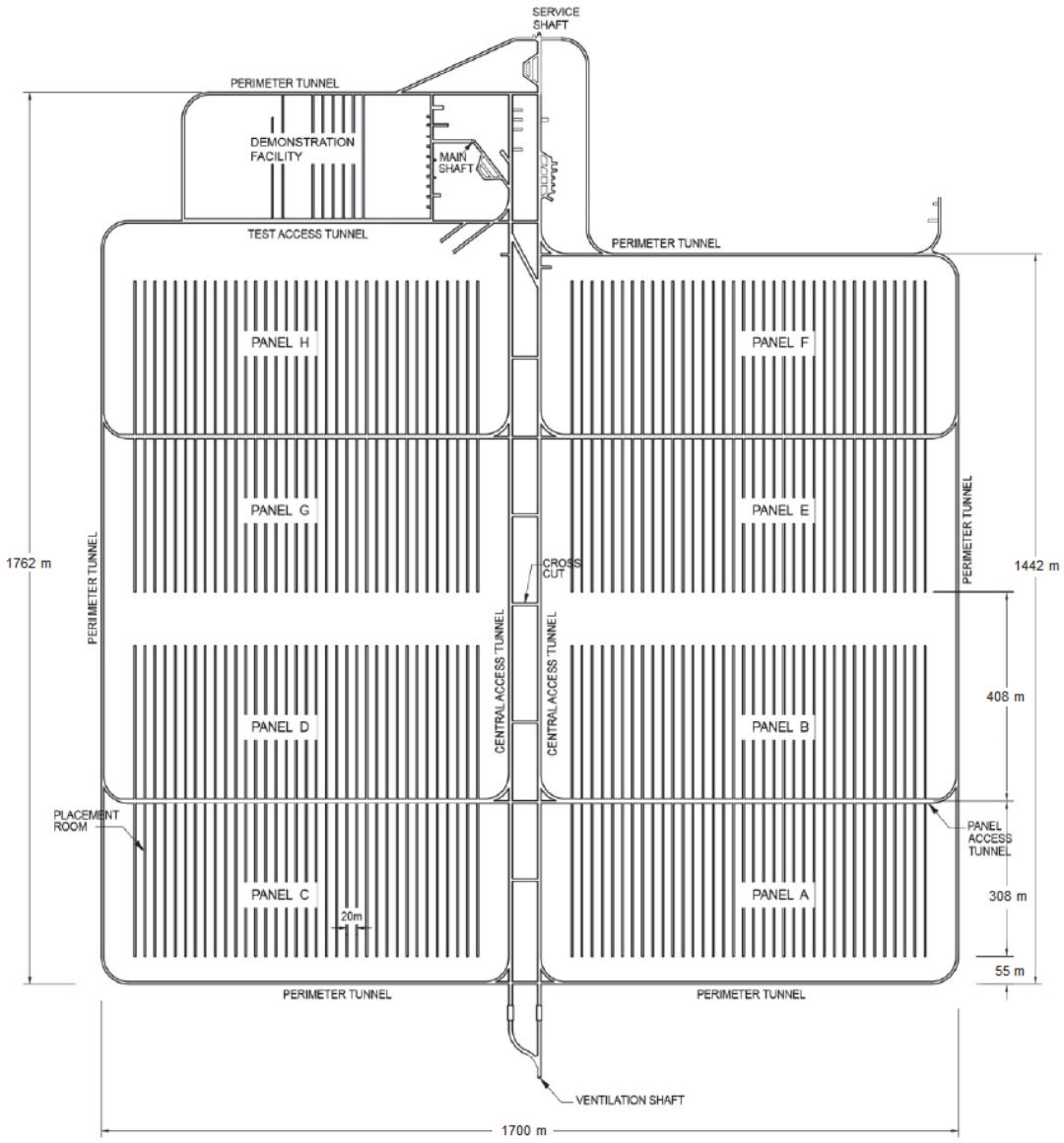

Figure 2: **Mark II Crystalline Underground Layout for 4.6 Million Bundles**

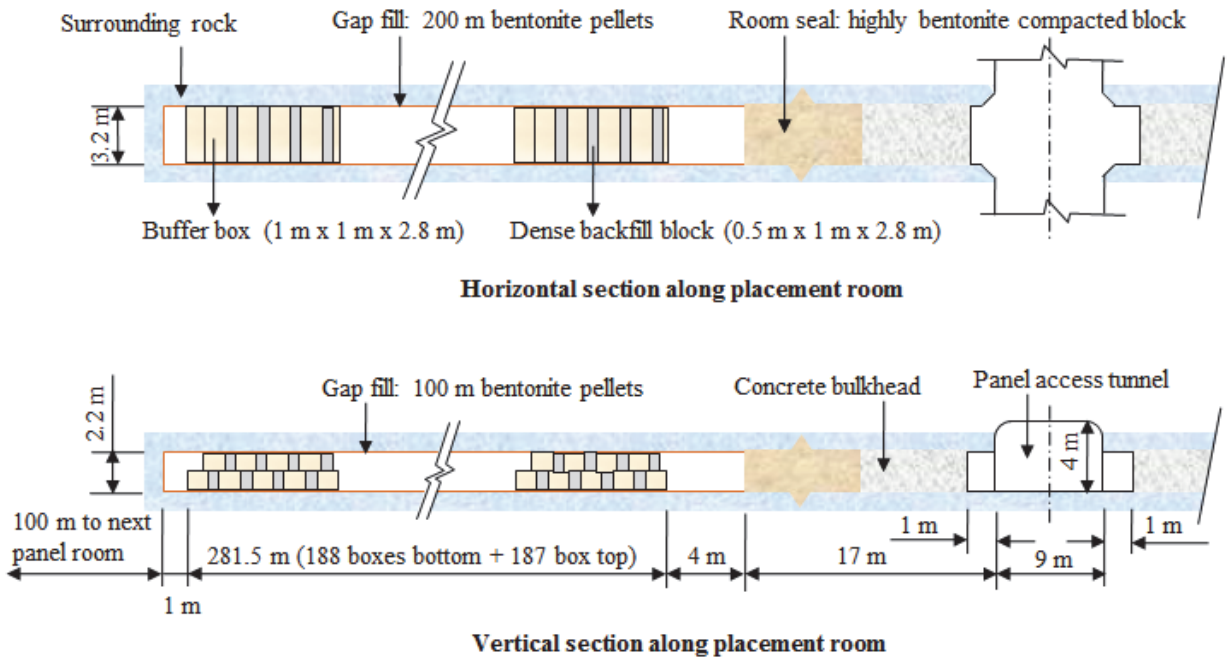

Figure 3: Plan View and Longitudinal Section of Placement Room

3. THEORY

This study is performed using COMSOL, which is a finite element analysis, solver and simulation software package for various physics and engineering applications, especially coupled phenomena, or multiphysics (COMSOL 2015a, 2015b).

3.1 THERMAL EQUATIONS

The following equation is used for thermal heat transfer in the rock (COMSOL 2015a).

$$\rho C_p \frac{\partial T}{\partial t} = \nabla \cdot (k \nabla T) + Q \tag{1}$$

Where ρ is the density, C_p is the heat capacity, k is the thermal conductivity, and Q is the heat source or sink. T is the temperature.

3.2 MECHANICAL EQUATIONS

The following equation is used for the mechanical response of the rock, including thermal effects (COMSOL 2015b)

$$\rho \frac{\partial^2 u}{\partial t^2} - \nabla \cdot \sigma = F_v \tag{2}$$

Where u is the deformation, σ is the stress tensor, F_v is the volume force.

$$\sigma - \sigma_0 = C : (\epsilon - \epsilon_0 - \epsilon_{inel}) \tag{3}$$

Where σ_0 is the initial stress, ϵ is the strain, ϵ_0 is the initial strain, C is the 4th order elasticity tensor, ":" stands for the double-dot tensor product (or double contraction), and ϵ_{inel} can be calculated using the following equation:

$$\epsilon_{inel} = \alpha(T - T_{ref}) \quad (4)$$

Where α is the thermal expansion coefficient, T_{ref} is the reference temperature.

The strain is calculated using the following equation:

$$\epsilon = \frac{1}{2}[(\nabla u)^T + \nabla u] \quad (5)$$

4. ASSUMPTIONS AND MATERIAL PROPERTIES

4.1 ASSUMPTIONS

Each of the repository materials is assumed to be homogeneous and isotropic with temperature-independent properties. The rock mass around the DGR is assumed infinite in horizontal extent.

4.2 MATERIAL PROPERTIES

USED-FUEL PROPERTIES

The heat output from the used fuel in each storage container is shown in Table 1 based on Tait et al. (2000). The fuel is assumed to have a burnup of 220 MWh/kgU and to undergo an initial cooling period of 30 years prior to placement. The DGR is assumed to be filled instantaneously with 30-year-out-of-reactor fuel at the reference conditions.

Table 1: Heat Output of a Container of Reference Used CANDU Fuel (220 MWh/kgU Burn-up) at Different Times

Time out-of-reactor (years)	Q per container (W/container) (48 bundles)	Time out-of-reactor (years)	Q per container (W/container) (48 bundles)
30	169	150	46.1
35	155	160	44.1
40	142	200	38.7
45	131	300	32.8
50	122	500	26.9
55	113	1000	18.7
60	105	2000	12.8
70	91.6	5000	9.24
75	85.9	10000	6.64
80	80.9	20000	3.84
90	72.3	35000	2.10
100	65.3	50000	1.32
110	59.8	100000	0.38
135	50.0	1000000	0.14

ROCK-MASS PROPERTIES

The material properties of the rock mass are based on measurements from Lac du Bonnet granite (Martin 1993). The rock has a thermal conductivity of 3.0 W/(m·°C) (Baumgartner 1995), a specific heat of 845 J/(kg°C) (Baumgartner 1995), a bulk density of 2700 kg/m^3, a Young's modulus of 50 GPa (Ikonen 2007), a Poisson ratio of 0.25 (Baumgartner 1995) and a thermal expansion coefficient of 1.0x10^{-5} °C^{-1} (Baumgartner 1995). Because the engineered sealing materials account for only a very small portion of the DGR and are thought to have a negligible impact on the thermal and mechanical response on the ground surface, they are not incorporated in this model.

An average convective heat transfer coefficient of 7.2 W/(m^2·°C) is applied on the ground surface (Garzolli and Blackwell 1981). This value is calculated at a wind velocity of 0 m/s from the following measured equation (Garzolli and Blackwell 1981).

$$h_0 = 7.2 + 3.8v \tag{6}$$

in which v is the air velocity, m/s; h_0 is the convective heat transfer coefficient, W/(m^2·°C).

Two lower values (i.e., 1 W/(m^2·°C) and 4 W/(m^2·°C)) are also used in sensitivity analyses to investigate the dependence of the ground surface temperature to the assumed convective heat transfer coefficient.

5. THE COUPLED THERMAL-MECHANICAL MODEL

This section describes the coupled thermal-mechanical model for a repository with a placement room spacing of 20 m (Figure 2) and a container spacing of 1.5 m in the same layer (Figure 3).

This repository has 284 placement rooms in eight panels, with four panels each having 35 placement rooms and four panels each having 36 placement rooms at a depth of 500 m from the ground surface (Figure 2). There are 375 buffer box positions available in each room. Conservatively, two 36 placement room panels with 375 containers in each room are chosen as the case for building the coupled thermal-mechanical model.

5.1 MODEL GEOMETRY, THERMAL BOUNDARY AND INITIAL CONDITIONS

This analysis provides an assessment of the thermal and mechanical responses of the rock mass near the ground surface.

5.1.1 Model Geometry

An isometric view of the model is shown in Figure 4. Due to symmetry, only a one-quarter section of the repository is modelled. The model is bounded vertically by the ground surface on the upper side and by a plane 10,000 m below the ground surface at the bottom. The horizontal dimensions of the model in the X- and Y-directions are 6,000 m x 6,000 m. These dimensions should be sufficient such that the thermal and mechanical response of the rock at the boundaries remains unaffected by the presence of the DGR during the simulation time period, as per Guo (2016). One-quarter of the DGR is represented by two panels with a 2 m thick plate of material generating heat. The horizontal dimensions of one DGR panel are 720 m x 281.5 m as shown in Figure 5 (720 m is from the number of placement rooms (36) times the room spacing of 20 m and 281.5 m is the portion of the placement room with containers as shown in Figure 3). The locations of each panel in the model are also shown in Figure 5.

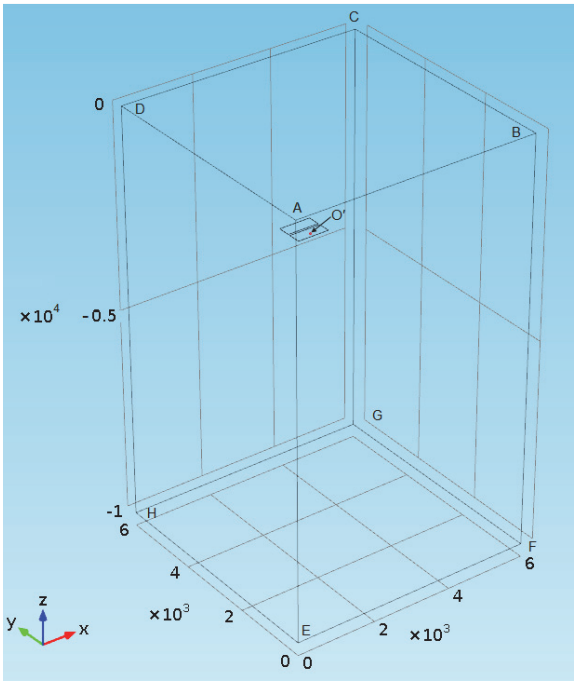

(Axis dimensions are in metres)

Figure 4: Isometric View of the Coupled Thermal-Mechanical Model

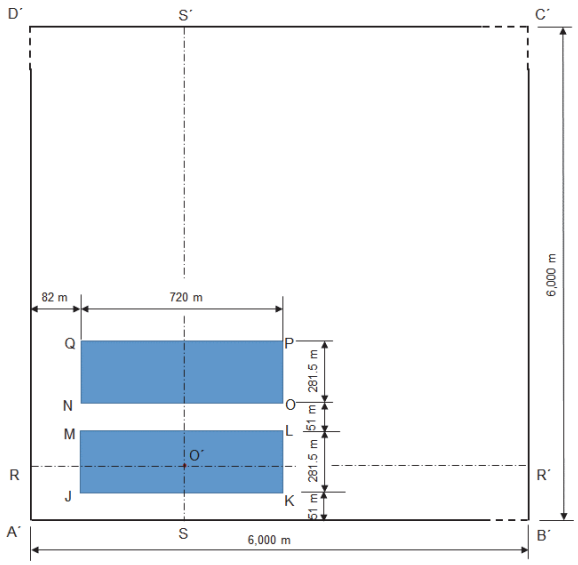

Figure 5: Cross Section of the Model at Depth of 500 m from the Ground Surface

5.1.2 Boundary Conditions

Thermal Boundary Conditions

The thermal boundary conditions are defined as follows.

- A convective heat flux boundary condition is applied on the top surface (Surface ABCE in Figure 4) of the model. The ambient air temperature is fixed at 5°C, representing the average Canadian Shield surface temperature (Baumgartner et al. 1995).
- The lower boundary (i.e., 10,000 m below ground surface) is also modelled as an isothermal boundary set at a temperature of 125°C (Baumgartner et al. 1995).
- The vertical boundaries are modelled as adiabatic planes of symmetry.
- The heat generated from the used-fuel containers in one-quarter of a repository is uniformly distributed throughout two panel plates (i.e., a rectangular plate of 720 m long by 281.5 m wide by 2.0 m high (2.0 m is the height of the two layers of buffer boxes)).

The model is representative of a finite size DGR positioned in an infinite extent of granite.

Mechanical Boundary Conditions

The mechanical boundary conditions are defined as follows:

- The vertical planes of the model are constrained not to move in the horizontal direction.
- The bottom plane of the model is fixed.
- The upper horizontal plane, the ground surface, is free to move.

5.1.3 Initial Conditions

Thermal Initial Conditions

The initial temperature of the model corresponds to a geothermal gradient of 0.012°C/m of depth, with the ground surface temperature at 5°C and the model bottom temperature at 125°C (Baumgartner et. al. 1995).

Mechanical Initial Conditions

The initial stresses and strains are set to 0. Due to the assumption that the rock mass is a linear elastic material, this has no influence on the thermally-induced displacement and stress calculation.

5.1.4 Finite Element Discretization

The finite-element discretization of the model is shown in Figure 6. The domain is discretized such that the elements are more densely distributed in the rock mass just above and beneath the repository level where the thermal gradients are expected to be the greatest. The model has 99,465 tetrahedral elements.

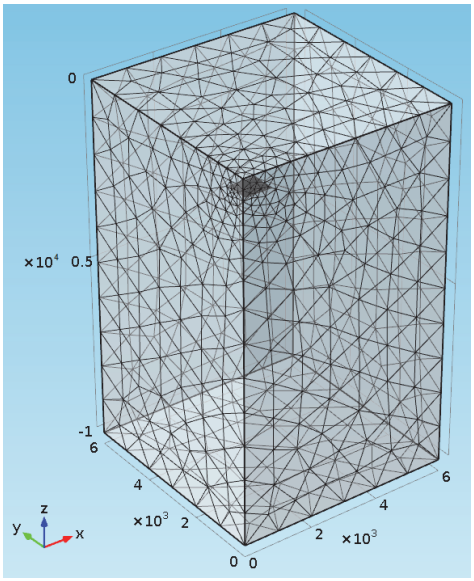

Figure 6: Mesh for the Coupled Thermal-Mechanical Model

5.2 NUMERICAL MODELLING RESULTS

This section presents the thermal and mechanical modelling results.

5.2.1 Thermal Results

Figure 7 and Figure 8 show an isometric view of temperature after 78 years and 700 years of used-fuel container placement. The temperature at repository level is 71°C (peak temperature) at 78 years and 67°C at 700 years at Point O´ (the original temperature is 11°C) (for location to see Figure 5). The temperature at the ground surface is very uniform and remains at about 5°C at 78 years and again at 700 years.

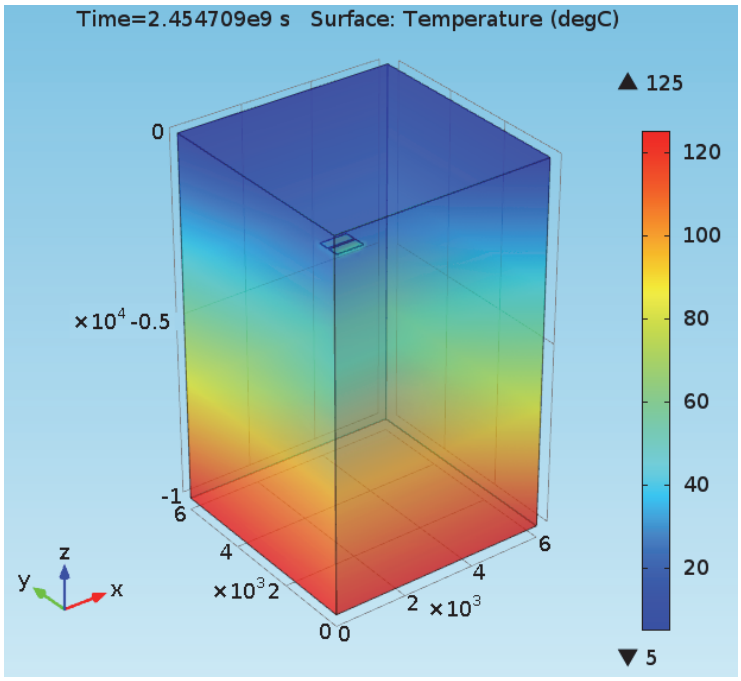

Figure 7: Isometric View of Temperature in the Model at 78 Years after Placement

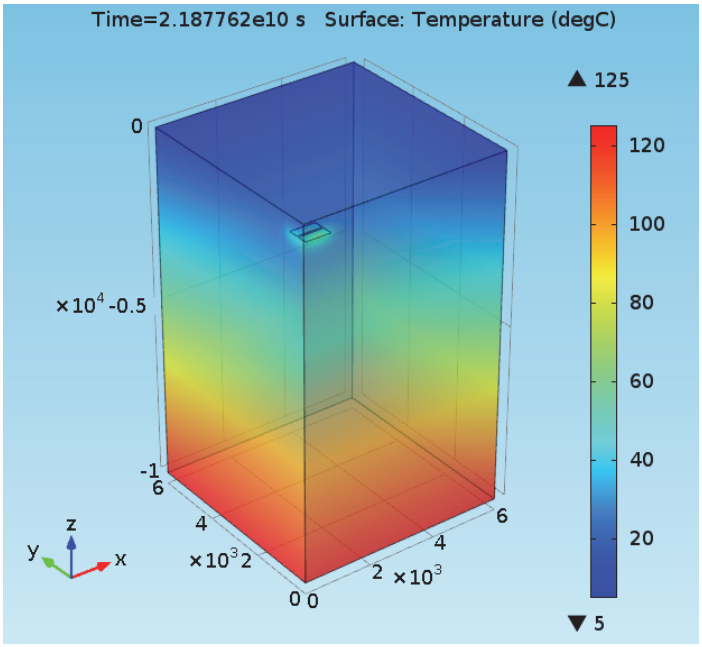

Figure 8: Isometric View of Temperature in the Model at 700 Years after Placement

To investigate the influence of the type of surface thermal boundary condition on the evolution of repository temperature, Figure 9 compares the modelled temperatures at location O´ (for location see Figure 5) for the case with a thermal convective boundary condition on the ground surface with the case with a fixed temperature (5°C) on the ground surface (described in Guo 2016). The comparison shows essentially no difference in temperature at the repository.

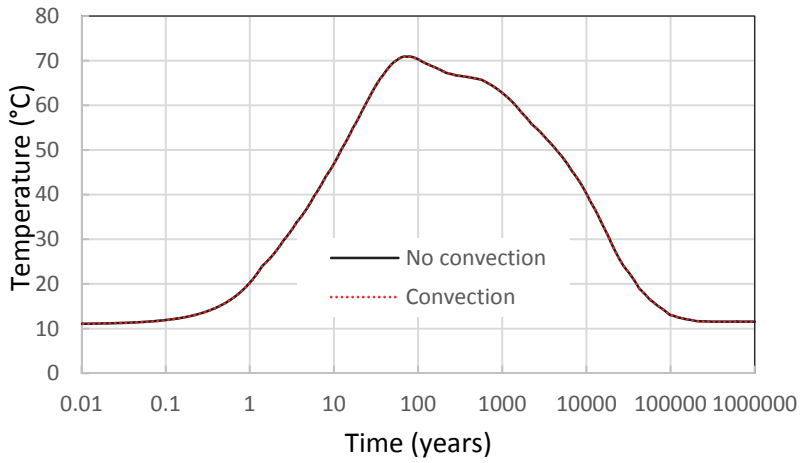

Figure 9: Temperature as a Function of Time at Panel Centre O′ from the Model

Figure 10 shows a close up view of the modelled temperature on the ground surface at a point just above the panel centre (O′) and at Point A (just above the repository centre) for the case

with the thermal convection boundary condition. The effect of the DGR on the ground surface temperature is negligible (i.e., less than 0.03°C).

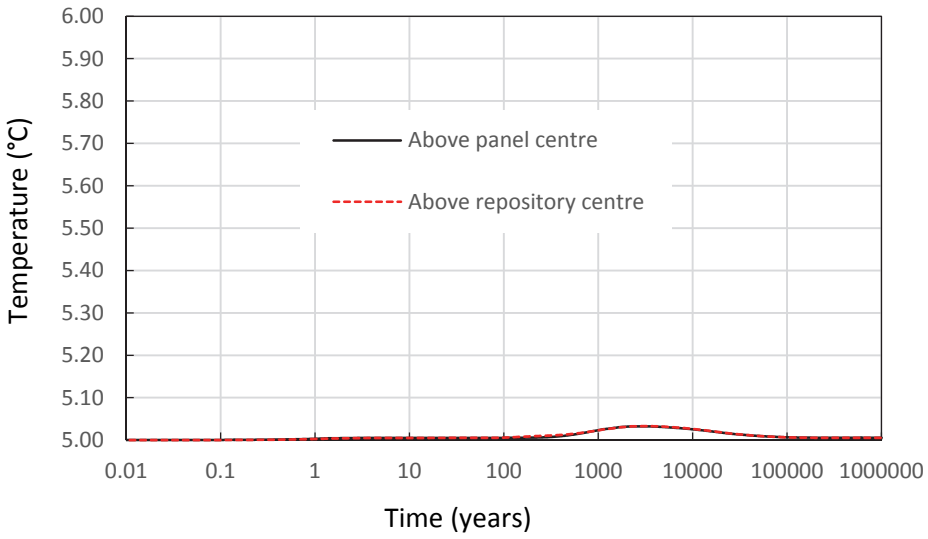

Figure 10: Temperatures at Ground Surface above the Repository Centre and the Panel Centre

Figure 11 shows the temperatures along the vertical line through the repository centre at different times. The thermal gradients along the vertical line are different near the ground surface, but the temperatures at the ground surface always converge to the ambient air temperature of 5°C.

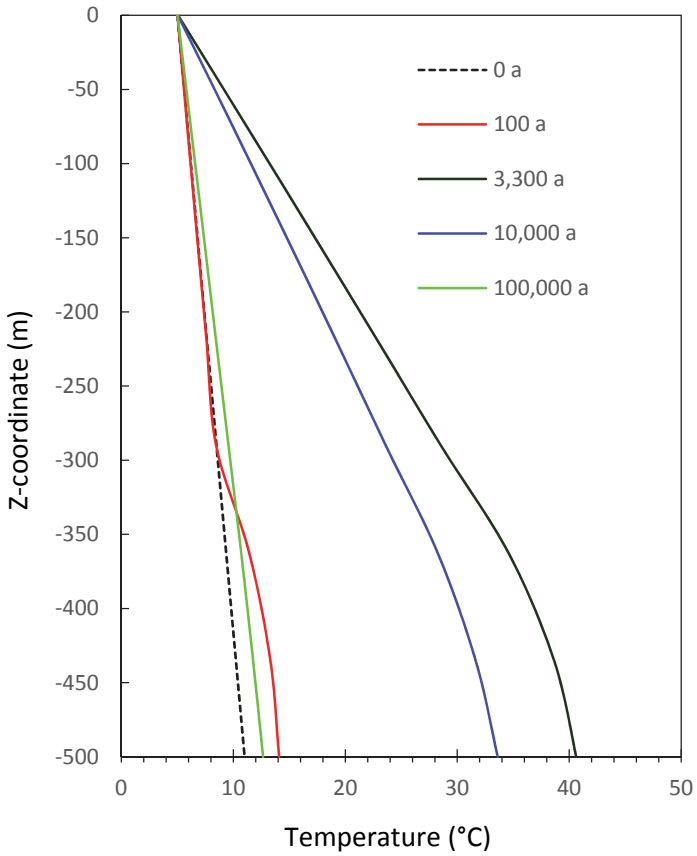

Figure 11: Temperature along the Vertical Line through the Repository Centre at Different Times

5.2.2 Mechanical Results

5.2.2.1 Thermally-Induced Displacement

Figure 12 shows the distribution of modelled maximum vertical displacements at ground surface occurring 3,400 years after used fuel placement. The maximum vertical displacement occurs at the point on the ground surface directly above the centre of the repository. The modelled uplift extends over an area larger than the repository footprint. The panel location is shown in the figure for context.

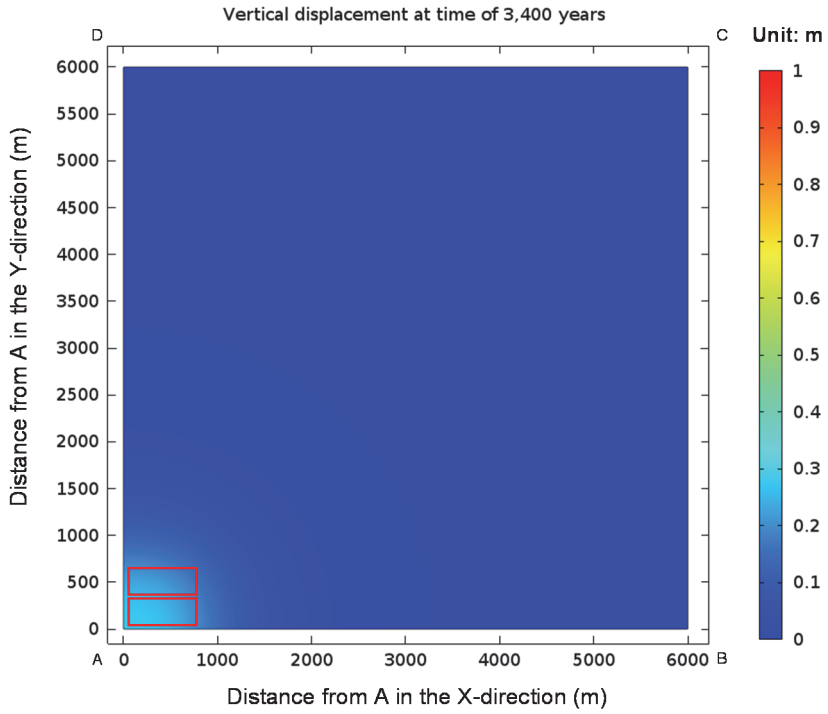

Figure 12: Vertical Displacement of the Ground Surface after 3,400 Years

Figure 13 shows the modelled vertical displacement as a function of time at the point on the ground surface above the repository centre. The maximum modelled uplift is 28 cm occurring at 3,400 years.

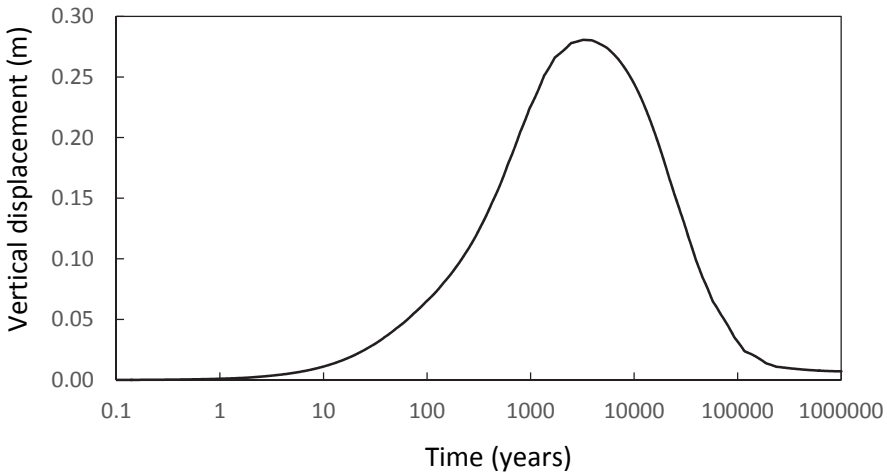

Figure 13: Modelled Vertical Displacement at the Point on the Ground Surface above the Repository Centre

Figure 14 shows the vertical displacement along vertical line AB (for location see Figure 4) on the ground surface at 3,400 years (i.e., at the time of peak displacement). At Point A (the point on the ground surface above the repository centre) the uplift is 28 cm. At a point 4,000 m from Point A the uplift approaches 0 cm. Posiva analysis (Ikonen 2007) assumes the same coefficient of thermal expansion and shows an uplift of 13.8 cm would occur for a thermal heat load of 3.42 MW. In the report of Carvalho and Steed (2012), the uplift for a repository (1,565 m x 2,001 m) hosting 3.6 million Candu bundles is 20 cm. Compared with these results, the 28 cm uplift for the conceptual repository in this study (1,442 m x 1,700 m and hosting 4.6 million Candu bundles) is comparable.

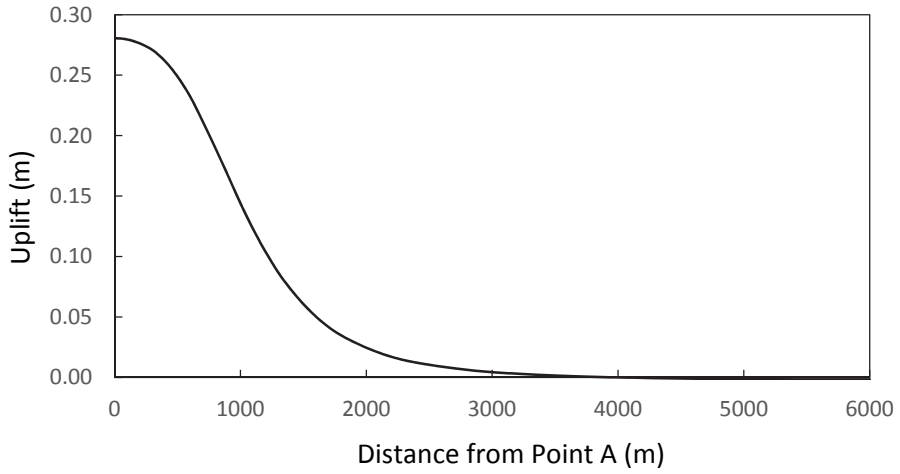

Figure 14: Vertical Displacement along Line AB on the Ground Surface at 3,400 Years

5.2.2.2 Thermally-Induced Stresses

Due to the presence of a heat-generating source, temperature changes in the rock give rise to thermal stresses, caused by thermal expansion of the rock mass. These thermally induced stresses are obtained by numerical simulation. Stresses in the X-direction and Y-direction are caused by the ground deformation associated with the vertical uplift. Figure 15 shows the thermally-induced stress at the ground surface above the repository centre when a thermal expansion coefficient of 1×10^{-5} °C^{-1} is used. The maximum thermally-induced tensile stresses are 11.8 MPa in the X-direction, occurring after 3,170 years and 13.6 MPa in the Y-direction occurring after 2,460 years (tensile stress is expressed as a positive quantity for this discussion). The maximum stresses occur when there is maximum curvature in the ground surface.

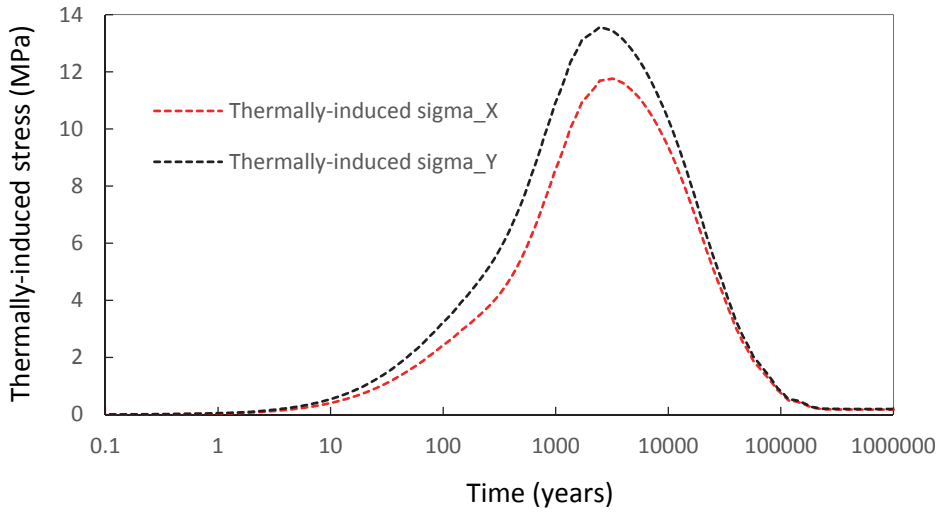

Figure 15: Thermally-Induced Stresses at Ground Surface above the Repository Centre

The simulated, thermally-induced, mechanical stresses are superimposed on the in-situ stresses as shown in Equation 7 to obtain the total stresses in the rock mass. The ambient in-situ stress, σ_1, is applied in the Y direction and the stress, σ_2, is applied in the X direction.

In accordance with Baumgartner et al. (1995), the ambient in-situ stresses for the relaxed domain from the ground surface to a depth of 300 m used in these analyses are as follows:

$$\begin{cases} \sigma_1 = -0.1345\ MPa/m \cdot depth - 18.5\ MPa \\ \sigma_2 = -0.1112\ MPa/m \cdot depth - 9.9\ MPa \\ \sigma_3 = \sigma_v = -0.026\ MPa/m \cdot depth \end{cases} \quad (7)$$

where σ_v is the vertical stress; and

σ_1, σ_2 and σ_3 are the major, intermediate and minor principal stresses, respectively.

The vertical stress ($\sigma_3 = \sigma_v$) is based on the gravity load of the overlying rock at a density of 2,650 kg/m^3. The values for the major (σ_1) and intermediate (σ_2) principal stresses are derived from the extremely high surface stresses measured at the Medika pluton (Martino 1993) extrapolated linearly to the stresses measured below Fracture Zone 2 at the Canadian Underground Research Laboratory (Baumgartner et al. 1995). These very high stress values, which correspond to the non-fractured granite, are chosen for this analysis because the Young's Modulus of 50 GPa corresponds to non-fractured granite.

Figure 16 shows the simulated total stresses at the ground surface above the repository centre which are obtained by superimposing the thermally-induced stresses on the in-situ stresses. The maximum tensile stress is 1.9 MPa occurring in the X-direction (tensile stress is positive and compressive stress is negative for this discussion). The compressive stress decreases due to thermal response. Over time, the repository thermal load decreases and therefore the

temperature in the rock decreases, the thermal expansion-induced tensile stress decreases, and the total stress increases (moves towards compressive stress).

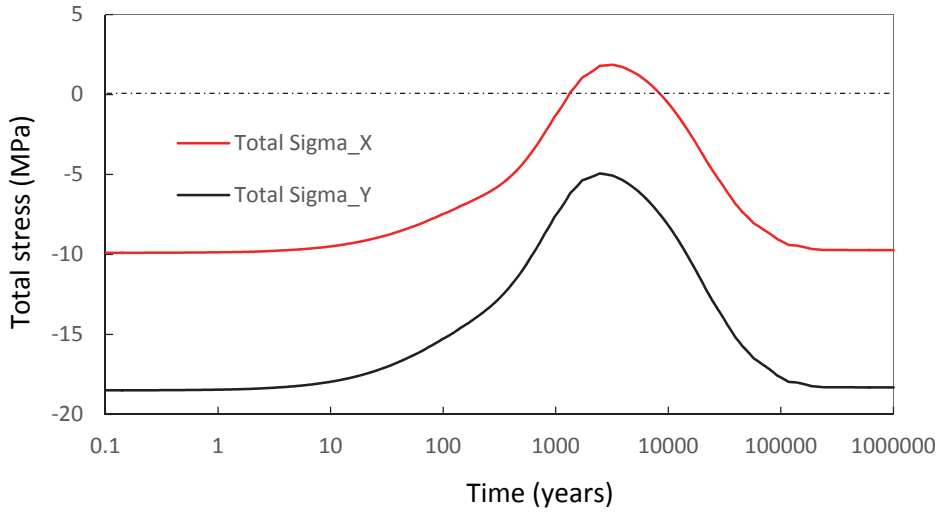

Figure 16: Total Stresses at Ground Surface above the Repository Centre Assuming Intact Rock Mass

Figure 17 shows the maximum depth of rock experiencing tensile stress from the ground surface with time. The tensile stress occurs between 1,300 years and 8,500 years. The maximum depth of rock with tensile stress (σ_x) is 11 m occurring 2,890 years after placement. In the report of Carvalho and Steed (2012), the maximum depth of rock experiencing tensile stress for a repository with dimensions of 1,565 m x 2,001 m and hosting 3.6 million Candu bundles is 50 m occurring about 2,000 years after placement. Compared with this value, the maximum depth of rock experiencing tensile stress is smaller in the current study. The reason for this is that in Carvalho and Steed (2012) a Young's modulus of 45 GPa (for intact granite) is used together with a lower initial stress from SNC-Lavalin (2011). In the current study, a Young's modulus of 50 GPa (for intact granite – see Section 4.2) is used together with a higher initial stress appropriate for intact rock (from Baumgartner et al. (1995)).

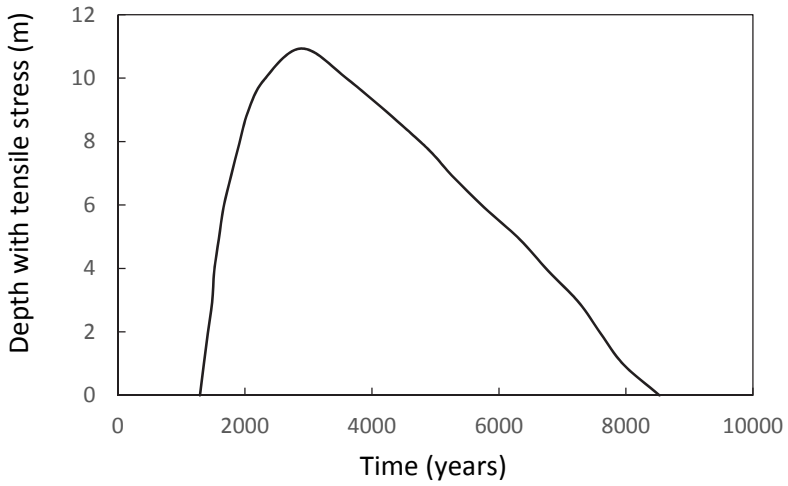

Figure 17: Tensile Stress Depth in Rock

The Hoek and Brown empirical failure criterion (Hoek and Brown 1980 and 1988) is adopted to evaluate the stability of the rock mass. The empirical equation of the Hoek and Brown failure criterion is given by:

$$\sigma_{1f} = \sigma_3 + (m \cdot \sigma_c \cdot \sigma_3 + s \cdot \sigma_c^2)^{\frac{1}{2}} \tag{8}$$

where σ_{1f} is the major principal stress at failure;

σ_3 is the minor principal stress;

σ_c is the uniaxial compressive strength of the intact rock materials from which the rock mass is made up; and

m and s are empirical constants.

There are two sets of parameters used in Hoek and Brown's failure criterion as first used by Baumgartner et al. (1995). The first set of parameters, applied during excavation, is for a condition below which no damage occurs to the rock. They are: m = 16.6, s = 1 and σ_c = 100 MPa. The second set of parameters is used for the peak strength of the undamaged rock under the full thermal-mechanical loads. These strength parameters can only be applied if the rock excavation stresses do not exceed the initial design parameters during excavation. They are: m = 25, s = 1 and σ_c = 150 MPa (Baumgartner et al. 1995).

For evaluation of the stability of the rock near the ground surface, the second set of parameters should be used to calculate the rock strength. For the rock near the ground surface, the minor stress is always the vertical stress and its value is zero. Therefore, the compressive strength should be the uniaxial compressive strength of the intact rock materials based on Equation (8):

$$\sigma_{1f} = \sigma_c = 150\ MPa \tag{9}$$

Granite tensile strength is about 4.8 MPa (from the website of www.EngineeringToolBox.com). Therefore, it is not possible to have tensile damage. Due to thermally-induced expansion, the compressive stress decreases and there is no possibility to have compressive damage either.

6. SENSITIVITY ANALYSES

This section studies the influence of:

- boundary conditions applied on the top surface;
- boundary conditions applied on the four vertical outside surfaces of the far-field model;
- Young's modulus used for the granite rock; and
- repository depth.

6.1 INFLUENCE OF THE THERMAL BOUNDARY CONDITION APPLIED ON THE TOP SURFACE

Figure 18 shows a comparison of temperatures at the ground surface directly above the repository centre obtained using different values of 1 W/(m^2·°C) and 4 W/(m^2·°C) rather than 7.2 W/(m^2·°C) for the convection heat transfer coefficient. The maximum difference is only 0.2°C between the case with 1 W/(m^2·°C) and the case with 7.2 W/(m^2·°C), indicating that results are not especially sensitive to the assumed value. The maximum difference is 0.03°C between the 4 W/(m^2·°C) case and the 7.2 W/(m^2·°C) case.

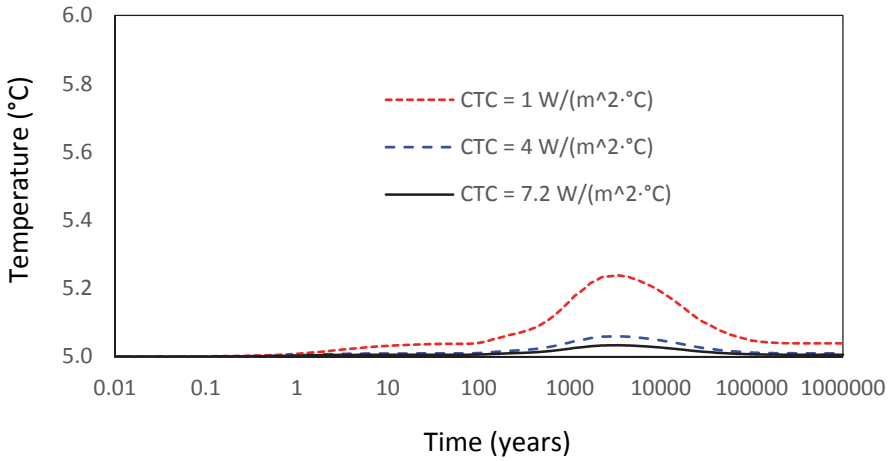

Figure 18: Influence of Convection Transfer Coefficient used in the Top Surface Boundary Condition

6.2 INFLUENCE OF THE MECHANICAL BOUNDARY CONDITION APPLIED ON THE VERTICAL BOUNDARIES IN THE FAR-FIELD MODEL

On Surfaces BCGF and CDHG (for location see Figure 4), a roller boundary condition (i.e., movement in the direction normal to the surface is not allowed) is applied. In this section the influence of different mechanical boundary conditions is investigated.

Figures 19, 20 and 21 show the comparison of the uplift, thermally-induced stresses in the X-direction and thermally-induced stresses in the Y-direction at the ground surface above the repository centre, as obtained from the far-field models using the roller boundary condition, a free boundary condition (i.e., movement in any direction is allowed) and a fixed boundary condition (i.e., movement in any direction is not allowed), respectively. Results show that the influence is negligible. This indicates that the horizontal dimensions are adequate for the purpose of this modelling study.

Results indicate that the mechanical boundary conditions applied on Surfaces BCGF and CDHG are not expected to have any thermal influence on the results.

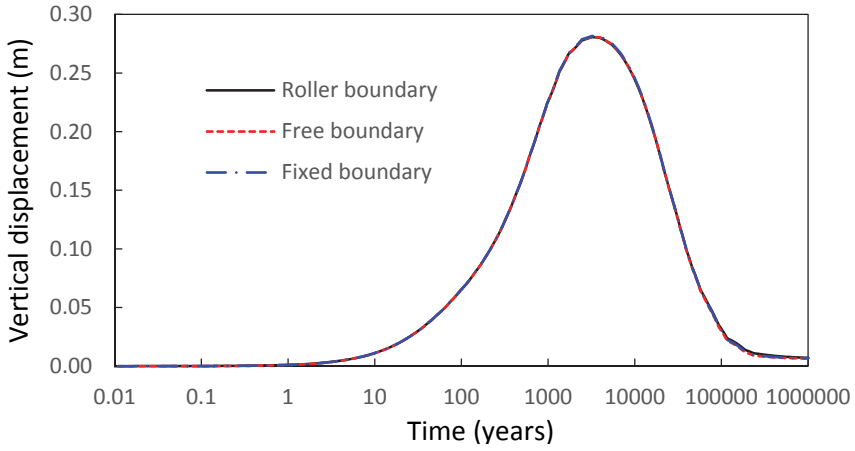

Figure 19: Comparison of the Vertical Displacement at the Ground Surface above the Repository Centre among Roller Boundary Condition, Free Boundary Condition and Fixed Boundary Condition applied on Surfaces BCGF and CDHG

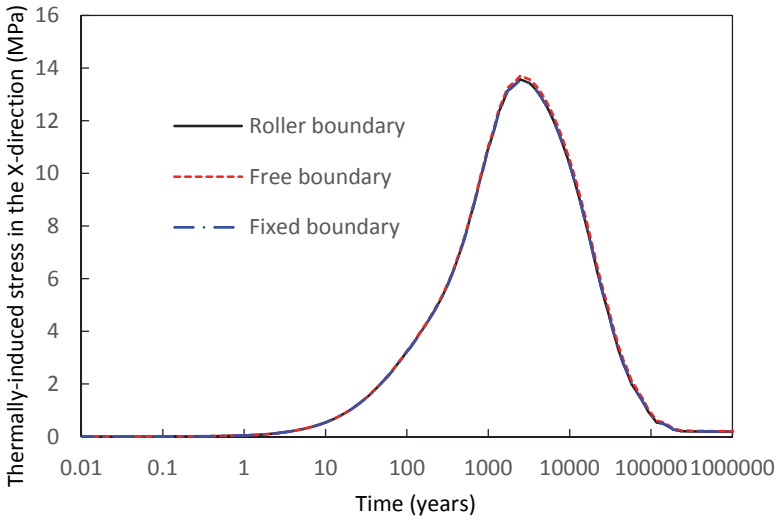

Figure 20: Comparison of the Thermally-induced Stress in the X-direction at the Ground Surface above the Repository Centre among Roller Boundary Condition, Free Boundary Condition and Fixed Boundary Condition applied on Surfaces BCGF and CDHG

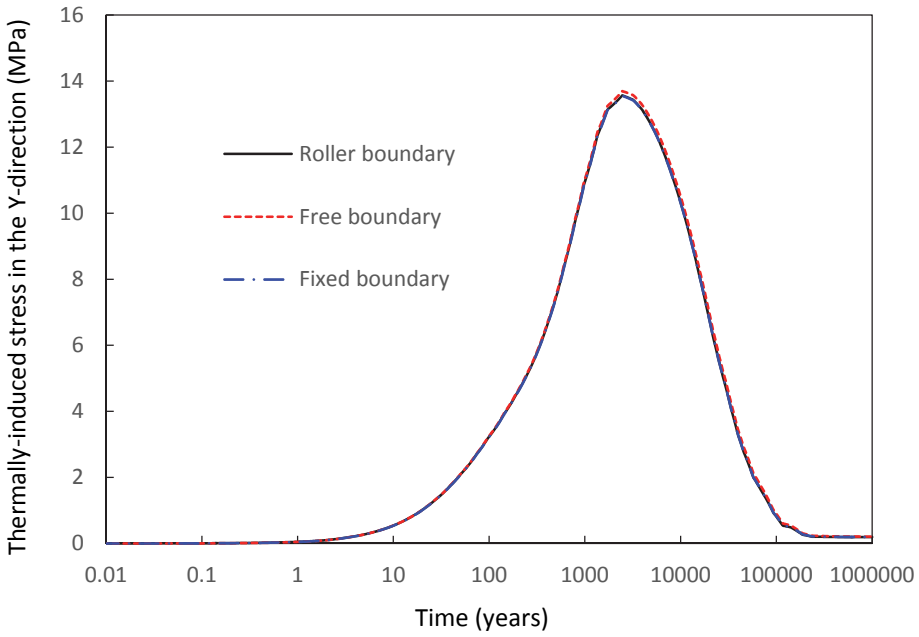

Figure 21: Comparison of the Thermally-induced Stress in the Y-direction at the Ground Surface above the Repository Centre among Roller Boundary Condition, Free Boundary Condition and Fixed Boundary Condition applied on Surfaces BCGF and CDHG

6.3 INFLUENCE OF YOUNG'S MODULUS

For the intact rock mass a Young's modulus of 50 GPa is used. However, near surface rock (from the ground surface to a depth of 150 m) may be fractured and have a lower effective Young's modulus (e.g., 25 GPa) (Ikonen 2007).

Figure 22 shows a comparison of the vertical displacement (uplift) at the ground surface above the repository centre using a Young's modulus of 50 GPa everywhere with that obtained using 25 GPa for the top 150 m and 50 GPa for deeper rock. The 25 GPa is appropriate for highly fractured rock. Results show that the simulated uplift of the ground surface above the repository when applying the 25 GPa value is 0.6 cm greater than otherwise. This is reasonable because the total vertical displacement is mainly dependent on the rock thermal expansion. The thermal expansion coefficients of the rock for two models are the same, and therefore the uplift results are similar.

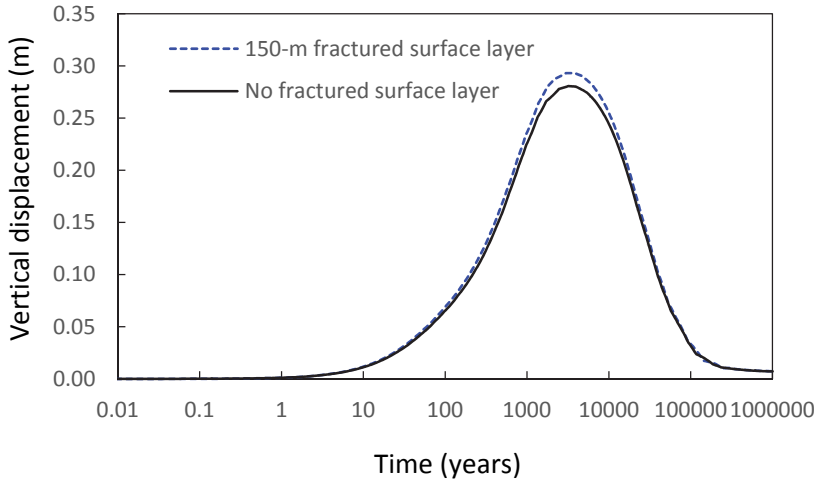

Figure 22: **Comparison of the Vertical Displacement at the Ground Surface above the Repository Centre between Considering and without Considering Fractured Layer**

There is also a significant reduction in stress at the ground surface. Figures 23 and 24 show the comparison of thermally-induced stresses in the X-direction and the Y-direction considering the fractured layer and without considering the fractured layer. The thermally-induced stresses in the X-direction and the Y-direction (when considering the fractured layer) are 6.7 MPa and 8.0 MPa, which are 57% and 59% of the stresses obtained without considering fractured layer.

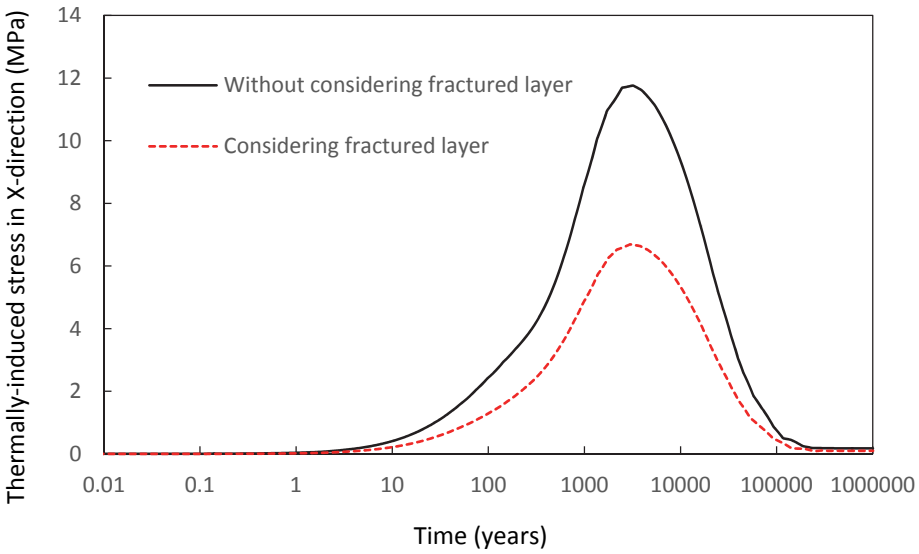

Figure 23: Comparison of the Thermally-induced Stress in the X-direction at the Ground Surface above the Repository Centre between using 50 GPa and 25 GPa as the Granite Young's Modulus

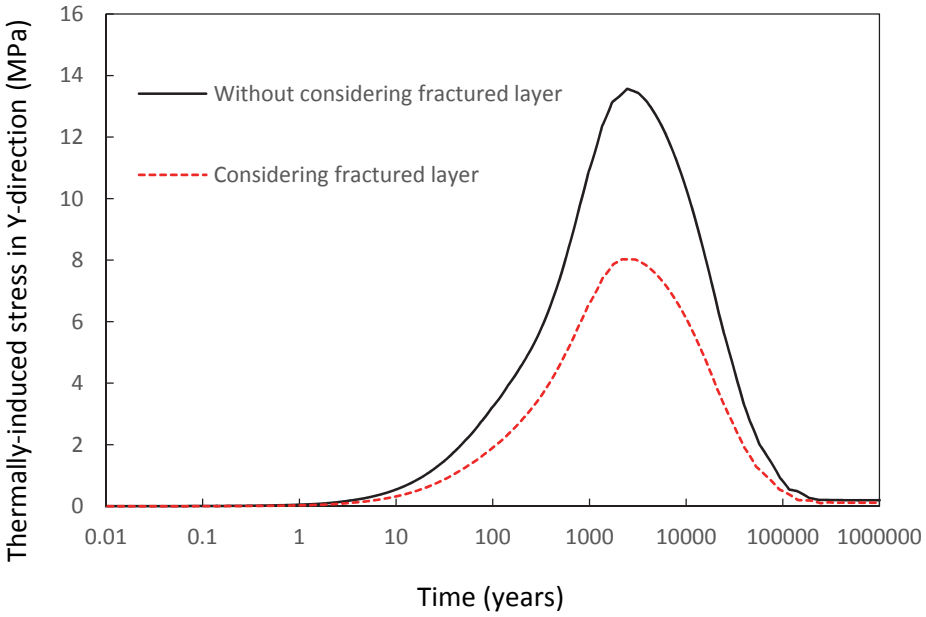

Figure 24: Comparison of the Thermally-induced Stress in the Y-direction at the Ground Surface above the Repository Centre between using 50 GPa and 25 GPa as the Granite Young's Modulus

If the top layer of rock with a thickness of 150 m is fractured, the in-situ stress should be smaller than that of the intact rock because the stress is relaxed or disturbed. Based on overcoring stress measurements from different places, Kaiser and Maloney (2005) give a best fit of the ambient in-situ stresses for the relaxed domain from the ground surface to a depth of 300 m as follows:

$$\begin{cases} \sigma_1 = -0.071\ MPa\ /\ m \cdot depth - 5.768\ MPa \\ \sigma_2 = -0.043\ MPa\ /\ m \cdot depth - 3.287\ MPa \\ \sigma_3 = -0.034\ MPa\ /\ m \cdot depth \end{cases} \quad (10)$$

The total stresses in the rock mass can be obtained by superimposing the simulated thermally induced mechanical stresses on the in-situ stresses as shown in Equation 10. The ambient in-situ stress, σ_1, is applied in the Y direction and the stress, σ_2, is applied in the X direction.

Figure 25 shows the total stresses at the ground surface above the repository centre which are obtained by superimposing the thermally-induced stresses on the in-situ stresses. The maximum tensile stress is 3.4 MPa occurring in X-direction 3,000 years after used fuel placement (tensile stress expressed as a positive value for this discussion). The compressive stress decreases due to thermal response.

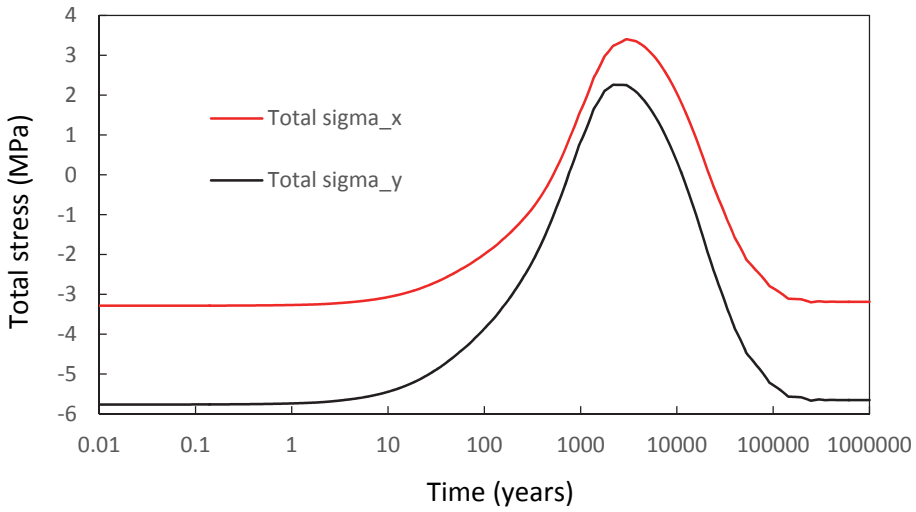

Figure 25: Total Stresses at Ground Surface above the Repository Centre Assuming the 150 m Top Layer of Rock Fractured

Figure 26 shows the maximum depth of rock experiencing tensile stress with time. The period of tensile stress occurs from 520 years to 21,500 years after used fuel placement. The maximum depth of rock with tensile stress (σ_x) is 45 m occurring 2,960 years after placement. This means that the fractures in the top 45 m layer of rock will be reactivated. Compared with the results from the model with intact rock, the tensile stress depth is much greater because the initial stress is a comparatively lower compressive stress due to the existence of fractures.

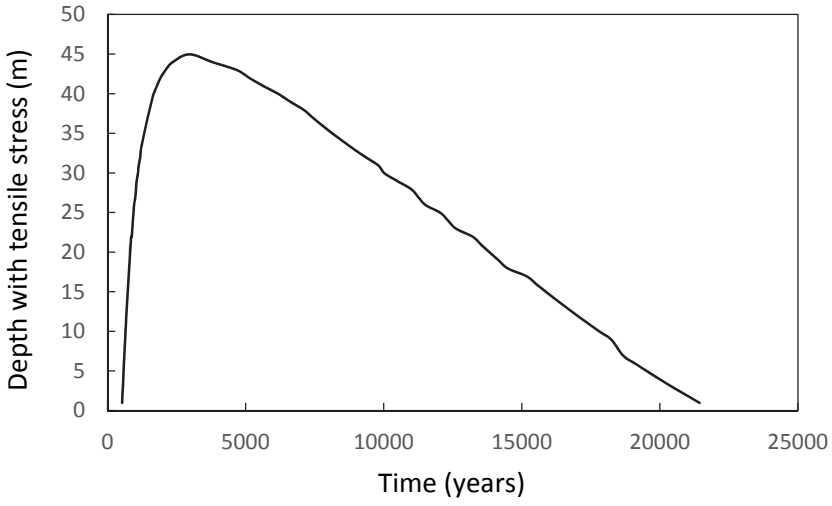

Figure 26: Tensile Stress Depth in Rock for the Case with the 150 m Top Layer of Rock Fractured

6.4 INFLUENCE OF REPOSITORY DEPTH

In this section the influence of repository depth is investigated.

Figure 27 shows a comparison of the uplift at the ground surface above the repository centre between a DGR located at a depth of 500 m and a DGR located at a depth of 600 m. The maximum uplift is 0.2 cm greater and occurs 1,300 years later for the repository at 600 m. The reason for this is that the greater depth means more rock is heated, with a corresponding lengthier period required for the full uplift to occur due to heat transfer.

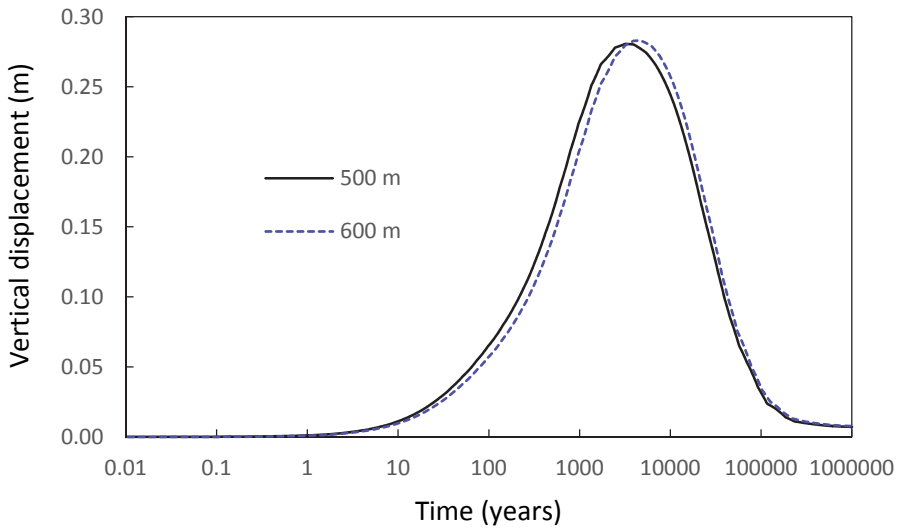

Figure 27: Comparison of the Vertical Displacement at the Ground Surface (Point A) between a DGR located at a Depth of 500 m and a DGR located at a Depth of 600 m

Figures 28 and 29 show a comparison of the thermally-induced stresses in the X-direction and Y-direction at the ground surface above the repository centre. As noted in Section 5.2.2.2, X- and Y-direction stresses are caused by ground deformation associated with the uplift, with the maximum values occurring at the time of maximum ground curvature.

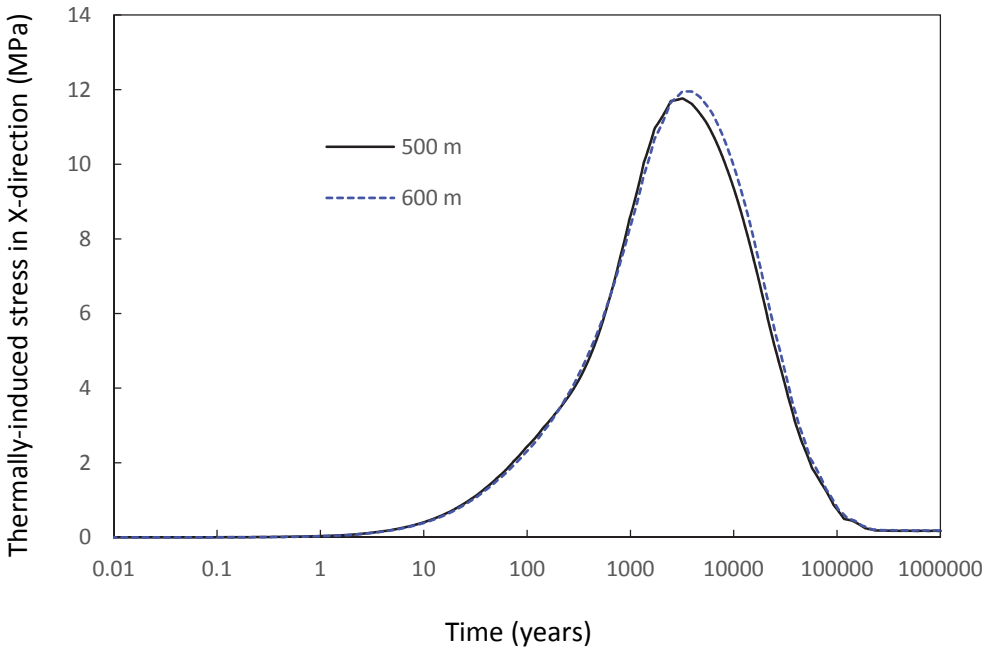

Figure 28: Comparison of the Thermally-induced Stress in the X-direction at the Ground Surface (Point A) between a DGR located at a Depth of 500 m and a DGR located at a Depth of 600 m

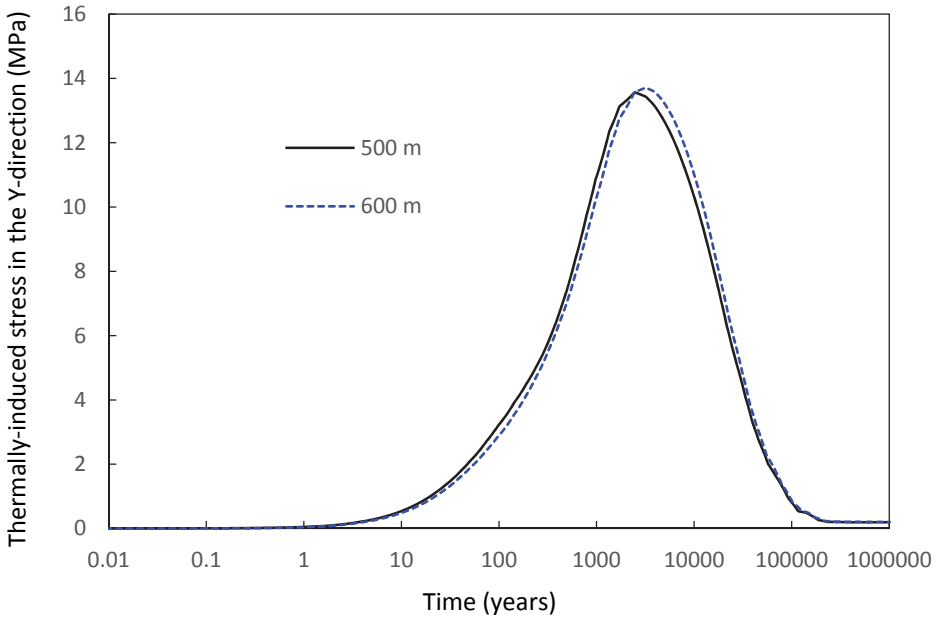

Figure 29: Comparison of the Thermally-induced Stress in the Y-direction at the Ground Surface (Point A) between a DGR located at a Depth of 500 m and a DGR located at a Depth of 600 m

7. SUMMARY AND CONCLUSIONS

A three-dimensional finite-element coupled thermal-mechanical analyses has been performed to gain a better understanding of the potential thermal and mechanical response in the rock near the ground surface.

A thermal convection boundary condition is used for the ground surface to investigate the thermal response. Results show that a DGR at a depth of 500 m in granite rock has a negligible effect on ground surface temperature.

The simulated, thermally-induced uplift of the ground surface above the repository centre is about 28 cm occurring 3,400 years after used fuel placement. The uplift is 2 cm at location up to a distance of 2 km from the point above the centre of the repository.

If the top 150 m layer of rock is fractured, the maximum uplift is about 28.6 cm occurring 3,400 years after used fuel placement.

The uplift results compare favorably with similar results from other modelling studies. Specifically:

- Posiva analysis (Ikonen 2007) assumes the same coefficient of thermal expansion and shows an uplift of 13.8 cm would occur for a thermal heat load of 3.42 MW. Given that the maximum heat load for the NWMO repository is 16.2 MW but spread over a larger area (1,442 m x 1,700 m), the 28 cm uplift value obtained in the current study is reasonably consistent.
- The report of Carvalho and Steed (2012) has an uplift of 20 cm for a repository of size (1,565 m x 2,001 m) hosting 3.6 million Candu bundles. This result also compares well with the 28 cm value obtained for the repository modelled in this report (i.e., (1,442 m x 1,700 m) with 4.6 million Candu bundles).

The simulated maximum depth of rock experiencing tensile stress is 11 m for the case with all intact rock, and about 45 m for the case with a 150 m overlying layer of fractured rock.

Increasing the depth of the DGR does not cause any significant change in the thermal and mechanical influence on the ground surface.

REFERENCES

Acres Consulting Services Limited in conjunction with RE/SPEC Ltd. 1985. A feasibility study of the multilevel vault concept. Atomic Energy of Canada Limited Technical Report, TR-297.

Acres Consulting Services Ltd. 1993. A preliminary study of long-hole emplacement alternatives. Atomic Energy of Canada Limited Technical Report, TR-346.

Baumgartner, P., D.M. Bilinsky, C. Onofrei, Y. Ates, F. Bilsky, J.L. Crosthwaite and G.W. Kuzyk. 1995. An in-room emplacement method for a used fuel disposal facility – preliminary design considerations. AECL Technical Record TR-665, COG-94-533. Chalk River, Ontario.

Baumgartner, P., T.V. Tran and R. Burgher. 1994. Sensitivity analyses for the thermal response of a nuclear fuel waste disposal vault. Atomic Energy of Canada Limited Technical Report, TR-621, COG-94-258.

Carvalho, J.L. and C.M. Steed. 2012. Thermal-mechanical analysis of a single level repository for used nuclear fuel. Nuclear Waste Management Organization APM-REP-00440-0010. (available at www.nwmo.ca).

COMSOL. 2015a. Heat Transfer Module User's Guide. Version COMSOL 5.1.

COMSOL. 2015b. Structural Mechanics Module User's Guide. Version COMSOL 5.1.

Garzoli, K.V. and J. Blackwell. 1981. An analysis of the nocturnal heat loss from a single skin plastic greenhouse. J. Agric. Eng. Res., 26: 203-214.

Golder Associates Ltd. 1993. Used-fuel disposal vault far-field thermal and thermalmechanical analysis. Atomic Energy of Canada Limited Report, TR-M-015.

Guo, R. 2007. Numerical modelling of a deep geological repository using the in-floor borehole placement method. Nuclear Waste Management Organization NWMO TR-2007-14. (available at www.nwmo.ca).

Guo, R. 2010. Coupled thermal-mechanical modelling of a deep geological repository using the horizontal tunnel placement method in sedimentary rock using CODE_BRIGHT. Nuclear Waste Management Organization NWMO TR-2010-22. (available at www.nwmo.ca)

Guo, R. 2016. Thermal response of a Mark II conceptual deep geological repository in crystalline rock. Nuclear Waste Management Organization NWMO-TR-2016-03. (available at www.nwmo.ca)

Hoek, E. and E.T. Brown. 1980. Underground Excavation In Rock. The Institute of Mining and Metallurgy, London.

Hoek, E. and E.T. Brown. 1988. The Hoek-Brown failure criterion – a 1988 update. 15th Canadian Rock Mechanics Symposium, Toronto, Canada.

Ikonen, K. 2007. Far-field thermal-mechanical response of one- and two-storey repositories in Olkiluoto. Posiva Working Report 2007-29.

Kaiser, P.K. and S. Maloney. 2005. Review of ground stress database for the Canadian Shield. Ontario Power Generation, Nuclear Waste Management Division 06819-REP-01300-10107-R00.

Martin, C.D. 1993. The strength of massive Lac du Bonnet granite around underground openings. Ph.D. Thesis, Department of Civil and Geotechnical Engineering, University of Manitoba, Winnipeg, Manitoba, Canada.

Mathers, W.G. 1985. HOTROK, a program for calculating the transient temperature field from an underground nuclear waste disposal vault. Atomic Energy of Canada Limited Technical Report, TR-366. **

Noronha, J. 2016. Deep geological repository conceptual design report crystalline / sedimentary rock environment. Nuclear Waste Management Organization APM-REP-00440-0015 R001. (Available at www.nwmo.ca).

SNC-Lavalin Nuclear Inc. 2011. APM conceptual design and cost estimate update – deep geological repository design report – crystalline rock environment – copper used fuel container. Prepared by SNC-Lavalin Nuclear Inc. for the Nuclear Waste Management Organization. APM-REP-00440-0001.

Tait, J.C., H. Roman and C.A. Morrison. 2000. Characteristics and radionuclide inventories of used fuel from OPG Nuclear Generating Stations. Volume 1 - Main report; and Volume 2 – Radionuclide inventory data. Ontario Power Generation Report 06819-REP-01200-10029-R00. Toronto, Canada.

Tsui, K.K. and A. Tsai. 1985. Thermal analyses for different options of nuclear fuel waste placement. Atomic Energy of Canada Limited Report, AECL-7823.